Inorganic Chemistry

Article

pubs.acs.org/IC

Cp*Co(III) Catalysts with Proton-Responsive Ligands for Carbon Dioxide Hydrogenation in Aqueous Media

Yosra M. Badiei,[†,⊥] Wan-Hui Wang,[‡,§,⊥] Jonathan F. Hull,[†] David J. Szalda,[†,∥] James T. Muckerman,*[,†] Yuichiro Himeda,*[,‡,§] and Etsuko Fujita*[,†]

[†]Chemistry Department, Brookhaven National Laboratory, Upton, New York 11973, United States

[‡]National Institute of Advanced Industrial Science and Technology, Tsukuba Central 5-2, 1-1-1 Higashi, Tsukuba, Ibaraki 305-8565, Japan

[§]Japan Science and Technology Agency, ACT-C, 4-1-8 Honcho, Kawaguchi, Saitama 332-0012, Japan

[∥]Department of Natural Science, Baruch College, CUNY, New York, New York 10010, United States

Supporting Information

ABSTRACT: New water-soluble pentamethylcyclopentadienyl cobalt(III) complexes with proton-responsive 4,4′- and 6,6′-dihydroxy-2,2′-bipyridine (4DHBP and 6DHBP, respectively) ligands have been prepared and were characterized by X-ray crystallography, UV−vis and NMR spectroscopy, and mass spectrometry. These cobalt(III) complexes with proton-responsive ligands predominantly exist in their deprotonated [Cp*Co(DHBP−2H$^+$)(OH$_2$)] forms with stronger electron-donating properties in neutral and basic solutions, and are active catalysts for CO_2 hydrogenation in aqueous bicarbonate media at moderate temperature under a total 4−5 MPa (CO_2:H_2 1:1) pressure. The cobalt complexes containing 4DHBP ligands ([**1**−**OH$_2$**]$^{2+}$ and [**1**−**Cl**]$^+$, where **1** = Cp*Co(4DHBP)) display better thermal stability and exhibit notable catalytic activity for CO_2 hydrogenation to formate in contrast to the catalytically inactive nonsubstituted bpy analogues [**3**−**OH$_2$**]$^{2+}$ (**3** = Cp*Co(bpy)). While the catalyst Cp*Ir(6DHBP)(OH$_2$)$^{2+}$ in which the pendent oxyanion lowers the barrier for H_2 heterolysis via proton transfer through a hydrogen-bonding network involving a water molecule is remarkably effective (*ACS Catal.* **2013**, *3*, 856−860), cobalt complexes containing 6DHBP ligands ([**2**−**OH$_2$**]$^{2+}$ and [**2**−**Cl**]$^+$, **2** = Cp*Co(6DHBP)) exhibit lower TOF and TON for CO_2 hydrogenation than those with 4DHBP. The low activity is attributed to thermal instability during the hydrogenation of CO_2 as corroborated by DFT calculations.

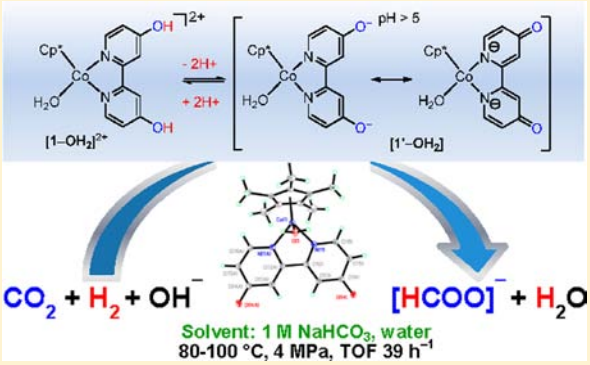

INTRODUCTION

Carbon dioxide is a greenhouse gas (GHG) that can retain the energy of absorbed sunlight and regulate the temperature of the atmosphere to sustain life on the planet. However, global climate concerns have arisen from the rapid increase of the atmospheric concentration of CO_2 produced from the escalating use of fossil fuels.[1,2] Only plants, through photosynthesis, can effectively utilize this plentiful and highly stable molecule on a massive scale for the synthesis of organic molecules. A long-standing goal is to develop efficient catalytic processes that mimic photosynthesis and selectively convert CO_2 to C1 building blocks and fuels.[3−5] Hydrogenation of CO_2 to formic acid (HCO_2H) and/or its conjugate base, formate (HCO_2^-), catalyzed by homogeneous transition-metal complexes is an important approach.[6−9] Hydrogen gas is a desirable fuel that can be utilized in fuel cells without the release of GHG; however, obstacles remain in finding practical means for its physical storage and transport.[3,10,11] Formic acid is a promising liquid hydrogen-storage material that takes advantage of the low energy barrier for CO_2 hydrogenation to formate in water (eq 1; $\Delta G^\circ = -4$ kJ mol^{-1}).[12−15] This strategy is also appealing because it avoids the formation of detectable levels of CO upon dehydrogenation of formic acid with transition-metal complexes under mild conditions, thereby preventing fuel cell catalyst poisoning.[16]

$$H_2 + CO_2 + OH^-(aq) \rightleftharpoons HCO_2^-(aq) + H_2O \quad (1)$$

High efficiencies and activities for the catalytic hydrogenation of CO_2 to formic acid in aqueous media have been achieved mainly using catalysts based on expensive noble metals such as Rh,[9,17] Ru,[18−21] and Ir,[22−26] and partially due to the high stability of their complexes in water. Nozaki et al. have reached unprecedented activities with a high turnover number (TON = 3.5×10^7), and a turnover frequency (TOF = 1.5×10^5 h^{-1}) at elevated temperatures (120 and 200 °C) and pressures (8 MPa) using a pincer PNP−Ir(III) complex.[27,28] Hazari and co-workers prepared a pincer-supported Ir(III) hydride species

Received: July 3, 2013
Published: October 16, 2013

   dx.doi.org/10.1021/ic401707u | *Inorg. Chem.* 2013, 52, 12576−12586

that can form a hydrogen bond with incoming CO_2 in the second coordination sphere;[23] however, the activity for CO_2 hydrogenation is rather comparable to the catalyst investigated by Nozaki et al. On the other hand, the development of efficient catalysts with nonprecious metals is also being pursued. In Inoue's pioneering work, a $Ni(dppe)_2$ catalyst (dppe = $Ph_2PCH_2CH_2PPh_2$) was found to be catalytically active, albeit with only a low TON of 7.[6] Using a combinatorial catalyst screening technique, Jessop et al. have obtained a TOF of 15 h^{-1} using $FeCl_3$ and $NiCl_3$ with phosphine ligands such as dcpe ($Cy_2PCH_2CH_2PCy_2$) or dppe in DMSO.[29] Recent success in CO_2 hydrogenation to formate with catalysts employing earth-abundant metals such as Fe[30,31] and Co[32] with tetradentate $P(CH_2CH_2PPh_2)_3$ has been demonstrated by Beller and co-workers. The best TOF and TON during 20 h runs in the latter Co system were reported to be 195 h^{-1} and 3877, respectively.[32] The reaction was carried out in an aqueous MeOH solution containing $NaHCO_3$ at 120 °C under high pressure (60 atm of H_2 measured at room temperature). The CO_2 hydrogenation system with $Co(dmpe)_2H$ (dmpe = 1,2-bis(dimethylphosphino)ethane) reported by Linehan et al. exhibits a remarkable TOF of 3400 h^{-1} at room temperature and 1 atm of 1:1 CO_2:H_2 (74 000 h^{-1} at 20 atm) in THF.[33] However, it is catalytic only when a superstrong base, Verkade's base (pK_a 33.7 in acetonitrile), was used essentially as a sacrificial reagent for the $Co(dmpe)_2H$ regeneration step. Milstein's PNP−Fe complex has been demonstrated to be a remarkably efficient iron catalyst, having a TOF and TON up to 156 h^{-1} and 788 at 80 °C under relatively low pressure (H_2, 6.6 atm and CO_2, 3.3 atm), although 2 M NaOH and 10% THF were added to increase the pH and the solubility of the complex, respectively.[34] Interestingly, the hydrido formate complex isolated in stoichiometric reactions in pentane was characterized by NMR and single-crystal X-ray diffraction. The reaction mechanism was predicted by theory.[35] While the observed activity shows a significant potential for the use of earth-abundant metal catalysts for the hydrogenation of CO_2, the search for high-performance low-cost catalysts in aqueous solutions under mild conditions still remains a challenging task.

While catalysts containing phosphine ligands are representative of a popular approach to CO_2 hydrogenation to formate, we have achieved high TONs and TOFs for CO_2 hydrogenation in water using proton-responsive half-sandwich Cp* iridium(III) complexes containing hydroxyl-substituted N-donor ligands (4,4′-dihydroxyl-2,2′-bipyridine (4DHBP), 6,6′-dihydroxyl-2,2′-bipyridine (6DHBP), 4,4′,6,6′-tetrahydroxyl-2,2′-bipyrimidine (THBPM), and 2,2′,6,6′-tetrahydroxyl-4,4′-bipyrimidine (TH4BPM); see Chart 1).[26,36−39] The high catalytic activities of the well-defined iridium(III) mononuclear $[Cp^*Ir(L)(OH_2)]^{2+}$ (L = 4DHBP, 6DHBP, TH4BPM) and dinuclear $[(Cp^*Ir)_2(L)(OH_2)_2]^{2+}$ (L = THBPM) complexes are attributed to the strong σ-electron-donating abilities of the ligands and improved water solubility by the high polarity of oxyanions generated from deprotonation of OH in basic solutions. Moreover, hydroxyl groups on ortho positions of the ligands (6DHBP, THBPM, and TH4BPM), acting as pendent bases, were found to accelerate the rate-limiting heterolysis of H_2 and consequently lead to dramatic rate enhancements.[37−39] We have, for the first time, obtained clear evidence from kinetic isotope effects (hydrogen and water) and computational studies of the involvement of a water molecule in the rate-determining heterolysis of H_2, and accelerated proton transfer by the formation of a water bridge in CO_2 hydrogenation in water.[38]

Chart 1. Structures of the Co and Ir Complexes Examined for CO_2 Hydrogenation

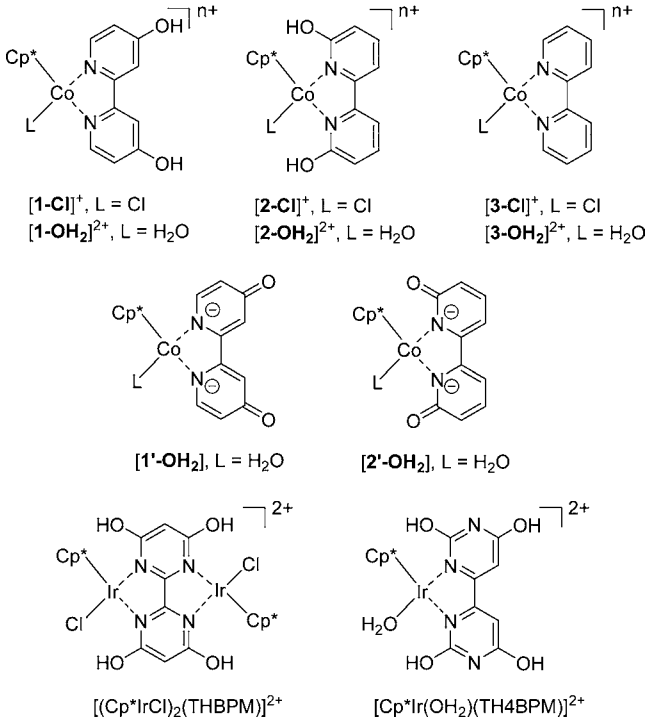

Remarkably, the dinuclear iridium catalyst containing the THBPM ligand exhibited excellent TOF (70 h^{-1}) in the reversible hydrogenation of CO_2 to formate at ambient temperature and pressure (25 °C, a total 1 atm H_2/CO_2, 1/1).[39] These findings demonstrate that the hydroxyl groups on the ligands play an important role in the hydrogenation of CO_2.

Given our success with the iridium(III) complexes bearing hydroxyl-substituted N-donor ligands, we envisaged the use of less expensive earth-abundant metals such as Co to replace the precious Ir metal in catalytic CO_2 hydrogenation. Cobalt-based catalysts are widely known for water reduction mediated by a Co(III) hydride species.[40,41] In contrast, as mentioned above, the only known well-defined homogeneous cobalt systems for CO_2 hydrogenation are the $[Co(H_2)(PP_3)]^+$ (PP_3 = P-$(CH_2CH_2PPh_2)_3$) species in water with $NaHCO_3$ reported by Beller et al.[32] and $Co(dmpe)_2H$ in THF reported recently by Linehan et al.[33] In the present study, we describe the preparation and characterization by UV−vis and NMR spectroscopy of new water-soluble Cp*Co(III) complexes, which bear dihydroxyl-substituted bipyridine (DHBP) ligands (Chart 1). Eight complexes were characterized by X-ray crystallography (Supporting Information Table S1). We also demonstrate, for the first time, the catalytic activity of these proton-responsive Co(III) complexes without any phosphine ligand toward hydrogenation of CO_2 in an aqueous bicarbonate medium without any organic cosolvent. Comparative structure−activity studies were also performed with the corresponding nonsubstituted analogues $[Cp^*Co(bpy)(L)]^{2+}$ (bpy = 2,2′-bipyridine) to assess the functional role of the hydroxyl substituents in catalytic CO_2 hydrogenation in 1 M $NaHCO_3$ aqueous solutions.

RESULTS AND DISCUSSION

Synthesis and Characterization of $[Cp^*Co(DHBP)(L)]^{n+}$ Complexes. As shown in the Supporting Information (Tables

dx.doi.org/10.1021/ic401707u | Inorg. Chem. 2013, 52, 12576−12586

S1−S14), a series of Cp*Co complexes with and without proton-responsive bpy ligands have been prepared, and their structures have been determined by X-ray diffraction. Complexes $[Cp^*Co(4DHBP)(Cl)]PF_6$ ($[\mathbf{1-Cl}]PF_6$) and $[Cp^*Co(6DHBP)(Cl)]PF_6$ ($[\mathbf{2-Cl}]PF_6$) were prepared by the reaction of the dichloro-bridged dimer $[Cp^*CoCl_2]_2$ and 2 equiv of DHBP ligand in a 1:3 mixture of water and methanol at 50 °C for 2 h (Supporting Information Scheme S1). The Cp*Co(III)DHBP complexes were isolated as air-stable purple crystals from saturated aqueous solutions of NH_4PF_6 in 72% and 61% yield for $[\mathbf{1-Cl}]PF_6$ and $[\mathbf{2-Cl}]PF_6$, respectively. The structure of $[\mathbf{1-Cl}]PF_6$ (**A**) crystallized from an aqueous solution and methanol was elucidated by single-crystal X-ray diffraction. This contains one water molecule and one methanol molecule of crystallization. As shown in Figure 1, the 18-electron Co(III) species $[\mathbf{1-Cl}]^+$ (**A**) exhibits a piano-stool geometry similar to the structurally related Ir(III) dihydroxyl-substituted bipyridine complexes[42,43] with a Co−Cl bond distance of 2.2917(6) Å and Co−N bipyridine distances [1.955(2) and 1.959(2) Å] typical of a Co(III) center (Table 1). The C−O bond distances found in $[\mathbf{1-Cl}]^+$ (**A**) of 1.340(2) and 1.338(2) Å indicate that the hydroxyl groups of the 4DHBP ligand remain protonated. The aqua complexes $[Cp^*Co(4DHBP)(OH_2)](PF_6)_2$ ($[\mathbf{1-OH_2}](PF_6)_2$) and $[Cp^*Co(6DHBP)(OH_2)](PF_6)_2$ ($[\mathbf{2-OH_2}](PF_6)_2$) were prepared in water via chloride ligand displacement by addition of $TlPF_6$ salt to $[\mathbf{1-Cl}]PF_6$ and $[\mathbf{2-Cl}]PF_6$, respectively. X-ray diffraction analysis of crystals harvested from a solution of $[\mathbf{1-Cl}]^+$ in 1 M $NaHCO_3$ (pH ≈ 8.4) revealed the formation of the neutral $[Cp^*Co(4DHBP-2H^+)(OH_2)]$ ($\mathbf{1'-OH_2}$) species. As shown in Figure 2, the X-ray structure of $\mathbf{1'-OH_2}$ exhibits the coordination of a water ligand to the cobalt center at a Co−O(1) distance of 1.952(2) Å. The shorter C−O bond distances (1.294(2) Å) found in $\mathbf{1'-OH_2}$ relative to those of $[\mathbf{1-Cl}]^+$ (**A**) (1.338(2) and 1.340(2) Å) are consistent with deprotonation of the hydroxyl groups of the 4DHBP ligand and the formation of the resonance-stabilized oxyanions under basic conditions (Scheme 1; Table 1). This acid−base equilibrium is similar to what has been observed for the structurally related Ir(III) DHBP systems.[22,39] Most notably, the deprotonated 4DHBP dianionic ligand in $\mathbf{1'-OH_2}$ is more planar than in $[\mathbf{1-Cl}]^+$ (**A**) and exhibits a larger dihedral angle between the Cp* centroid and 4DHBP ligand (38.45(9)° in $[\mathbf{1-Cl}]^+$ (**A**) and 60.03(7)° in ($[\mathbf{1-OH_2}]^{2+}$). The intra- and intermolecular H-bonding network in $\mathbf{1'-OH_2}$ involving water molecules (coordinated and uncoordinated) with the oxyanions is shown in Figure 3.

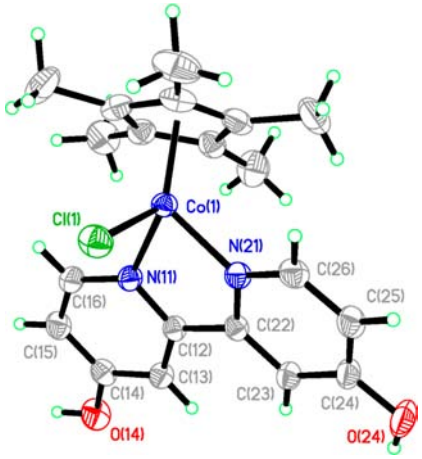

Figure 1. The crystal structure of $[\mathbf{1-Cl}]^+$ (**A**) crystallized from water and methanol as a cosolvent. The counterion (PF_6^-), methanol, and water molecules are not shown for clarity.

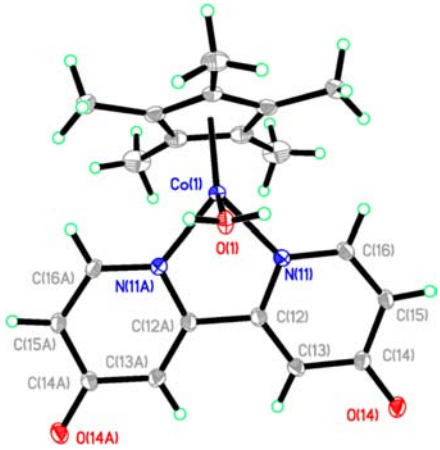

Figure 2. The crystal structure of $\mathbf{1'-OH_2}$ crystallized from dissolution of $[\mathbf{1-Cl}]^+$ in bicarbonate aqueous solutions (1 M $NaHCO_3$).

Table 1. Summary of Bond Distances (Å) and Angles (deg) for Complexes $[\mathbf{1-Cl}]^+$ (A) and $\mathbf{1'-OH_2}$

complex:	$[\mathbf{1-Cl}]^+$ (**A**), X = Cl	$\mathbf{1'-OH_2}$, X = O
protonation state:	4DHBP	4DHBP−2H$^+$
Bond Distances		
Co(1)−N(11)	1.959(2)	1.965(1)
Co(1)−N(21)	1.955(2)	1.965(1)
Co(1)−X(1)	2.2917(6)	1.952(2)
C(14)−O(14)	1.338(2)	1.294(2)
C(24)−O(24)	1.340(2)	1.294(2)
Bond Angles		
N(11)−Co(1)−N(21)	81.2(6)	82.33(7)
N(11)−Co(1)−X(1)	93.66(5)	87.68(5)
N(21)−Co(1)−X(1)	92.18(5)	87.68(5)

The X-ray structure of the $[Cp^*Co(6DHBP)(Cl)]BAr^F$ ($[\mathbf{2-Cl}]BAr^F$ complex crystallized from a solution of dichloromethane and hexane by exchanging the PF_6 counterion with BAr^F (BAr^F = tetrakis[3,5-bis(trifluoromethyl)phenyl]borate) was also determined. The structure shown in Figure 4 resembles the bond distances and angles found in $[\mathbf{1-Cl}]PF_6$ and a recently characterized iridium(III) analogue[43] (see Supporting Information experimental section for details). The C−O bond distances found in $[\mathbf{2-Cl}]^+$ of 1.332(7) and 1.339(8) Å, and the hydrogen bonding indicate that the hydroxyl groups of the 6DHBP ligand remain protonated. Strong hydrogen-bonding interactions were found in the case of $[\mathbf{2-Cl}]BAr^F$ between the chloride ligand and the *ortho*-hydroxyl pendent base groups of the 6DHBP ligand, which appears more geometrically distorted than the case of $[\mathbf{1-Cl}]^+$.

Furthermore, the X-ray structures of the $[\mathbf{1-Cl}]PF_6$ (**B**) and the acetonitrile adduct $[Co(6DHBP-H^+)(NCCH_3)]PF_6$ (6DHBP−H$^+$ = monodeprotonated 6DHBP) were obtained from the crystallization of $[\mathbf{1-Cl}]PF_6$ (**A**) and $[\mathbf{2-Cl}]PF_6$ complexes, respectively, from CH_3CN. ^{1}H NMR immediately

dx.doi.org/10.1021/ic401707u | *Inorg. Chem.* 2013, 52, 12576−12586

Scheme 1. Acid–Base Equilibrium between Complexes $[1{-}OH_2]^{2+}$ and $1'{-}OH_2$

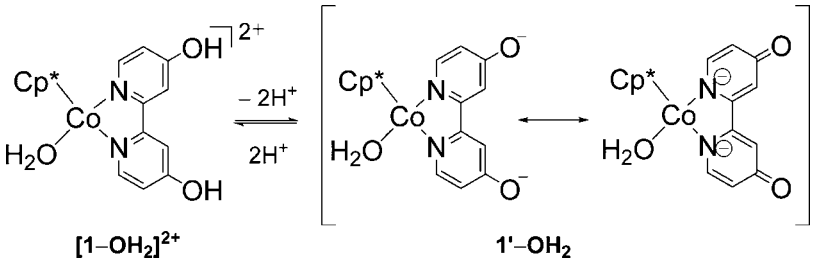

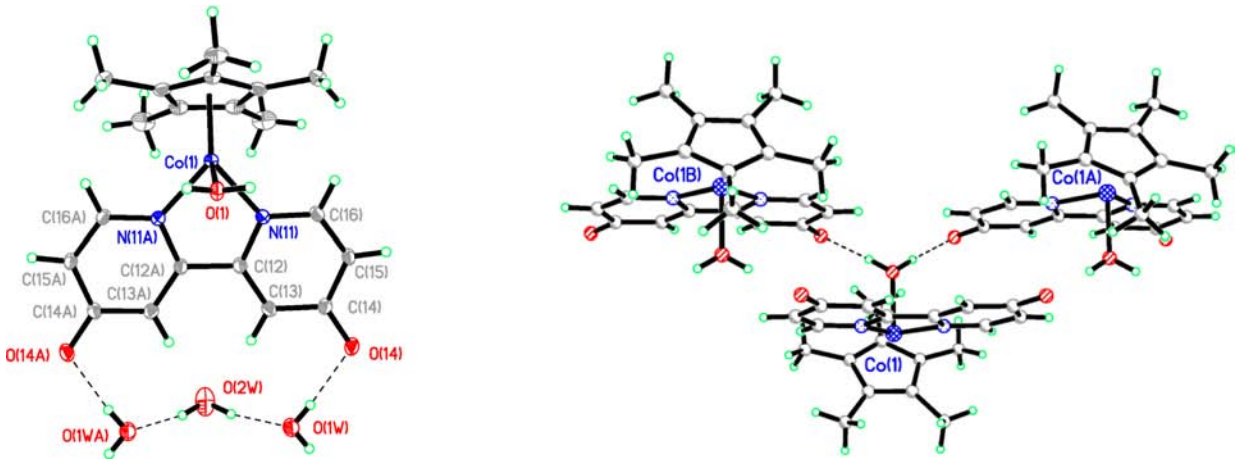

Figure 3. The hydrogen-bonding schemes in $[1'{-}OH_2]$ (left, intra-; right, intermolecular water bridged H-bonding interactions) between water and the two deprotonated hydroxyl groups of the 4DHBP ligand.

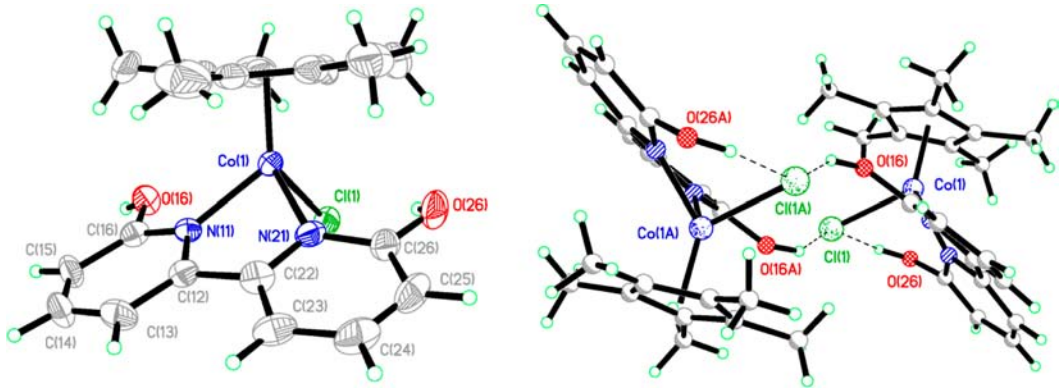

Figure 4. Left: The crystal structure of $[2{-}Cl]BAr^F$ crystallized from methylene chloride and hexane. The counterion (BAr^F) is not shown for clarity. Right: A view of the hydrogen bonding. Co(1A) is related to Co(1) by $2 - x$, $2 - y$, $1 - z$. The two rings of the bipyridine ligand exhibit a dihedral angle of 16.3(4)° to form the intramolecular and intermolecular hydrogen bond with the chloride ligand.

after preparation of a 1 mM solution of $[2{-}Cl]^+$ in CD_3CN shows the rapid exchange of the chloride with acetonitrile and the formation of $[Co(6DHBP{-}H^+)(NCCH_3)]^+$, although slower ligand exchange was observed in the case of $[1{-}Cl]^+$ (Supporting Information Figures S16 and S17). We also structurally characterized $[3{-}Cl]PF_6$, $[3{-}Cl]SO_3CF_3$, and a decomposition product $[Co(4DHBP{-}H^+)_2(4DHBP)]_3[Co(4DHBP)_3](PF_6)_6$ (**1d**) (where $4DHBP{-}H^+$ indicates monodeprotonated 4DHBP) isolated from aqueous solutions (vide infra). The results of all of the collected X-ray structures are described in detail in the Supporting Information (Tables S1–S14 and Figures S1–S10).

Acid–Base Equilibrium. The pK_a of the aqua complex $[1{-}OH_2](PF_6)_2$ was determined from the inflection points of sigmoidal least-squares fitted curves of the UV–vis spectra of the complex between pH 2–14 (Figure 5). The average pK_a value of the hydroxyl protons in $[1{-}OH_2]^{2+}$ is $pK_{a1+2} = 5.3$. In addition, we observed changes in the spectrum above pH 10 [$pK_{a(OH2)} \approx 11$], which are attributed to the deprotonation of the coordinated aqua complex. These pK_a values are quite similar to those found previously for the $[Cp^*Ir(4DHBP)(OH_2)]^{2+}$ complex ($pK_{a1+2} = 5.0$)[37] and imply that the metal does not appear to significantly influence the acidity of the DHBP ligand or the coordinated water molecule.[44] Curiously, the higher pK_a of the aqua ligand in complex $[1{-}OH_2]^{2+}$ ($pK_a \approx 11$) relative to that of the unsubstituted bpy complex $[Cp^*Co(bpy)(OH_2)]^{2+}$ $[3{-}OH_2]^{2+}$ ($pK_a \approx 8.4$)[44] is perhaps due to a contribution from the more electron-donating

dx.doi.org/10.1021/ic401707u | Inorg. Chem. 2013, 52, 12576–12586

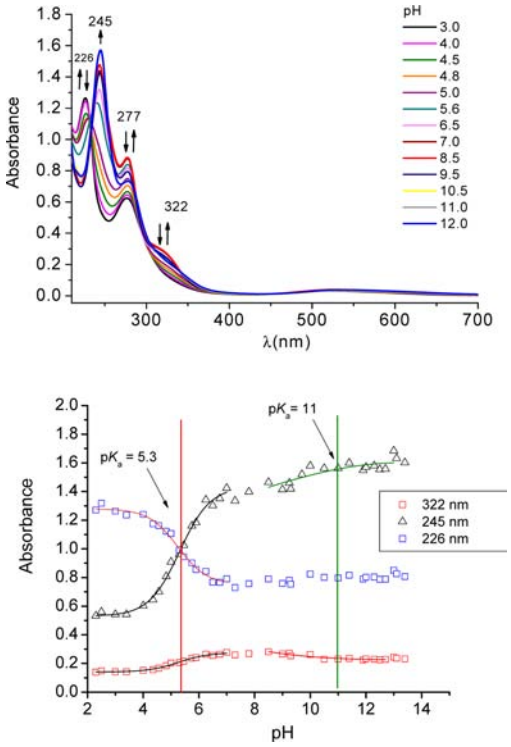

Figure 5. Acid–base pH titration of $[\mathbf{1}{-}\mathbf{OH_2}]^{2+}$ in 20 mM Britton–Robinson buffer between pH 3–12. Top panel: UV–vis spectral changes. Bottom panel: Absorbance changes at single wavelengths (322, 245, and 226 nm).

deprotonated DHBP and possible H-bonding interactions between the coordinated water and the oxyanions of other cobalt units in basic media as found in the X-ray structure.

Structural elucidation data for the complexes $[\mathbf{1}{-}\mathbf{Cl}]^{+}$, $[\mathbf{1}{-}\mathbf{OH_2}]^{2+}$, $[\mathbf{2}{-}\mathbf{Cl}]^{+}$, and $[\mathbf{2}{-}\mathbf{OH_2}]^{2+}$ were also obtained by ^{1}H NMR in D_2O, UV–vis, ESI/MS, and elemental analysis (see the Experimental Section and the Supporting Information for details). The comparative UV–vis spectra of complexes $[\mathbf{1}{-}\mathbf{OH_2}]^{2+}$, $[\mathbf{2}{-}\mathbf{OH_2}]^{2+}$, and $[\mathbf{3}{-}\mathbf{OH_2}]^{2+}$ in water are shown in Supporting Information Figure S12. At neutral pH, these cobalt complexes exhibit visible absorption bands between 530 and 550 nm with similar molar absorption coefficients (ε = 750–940 M^{-1} cm^{-1}). Complex $[\mathbf{2}{-}\mathbf{OH_2}]^{2+}$ displays an intense UV band absorption at lower energy (λ = 355 nm, ε = 10 550 M^{-1} cm^{-1}) as compared to $[\mathbf{1}{-}\mathbf{OH_2}]^{2+}$ and $[\mathbf{3}{-}\mathbf{OH_2}]^{2+}$ possibly due to a ligand-to-metal charge-transfer (LMCT) arising from the strong electron-donating nature of the deprotonated DHBP ligand and some influence of pendent bases near the Co center. A similar trend has been observed in the analogous Ir complexes.[37,43] In basic solutions (1 M $NaHCO_3$, pH 8.4), the UV–vis features of the Co DHBP complexes ($[\mathbf{1}{-}\mathbf{Cl}]^{+}$, $[\mathbf{1}{-}\mathbf{OH_2}]^{2+}$, $[\mathbf{2}{-}\mathbf{Cl}]^{+}$, and $[\mathbf{2}{-}\mathbf{OH_2}]^{2+}$) are practically the same as the corresponding spectra obtained in neutral water. Although all of the cobalt complexes ($[\mathbf{1}{-}\mathbf{Cl}]^{+}$, $[\mathbf{1}{-}\mathbf{OH_2}]^{2+}$, $[\mathbf{2}{-}\mathbf{Cl}]^{+}$, and $[\mathbf{2}{-}\mathbf{OH_2}]^{2+}$) have distinguishable chemical shifts in D_2O (Supporting Information Figures S13 and S14) indicating that the metal–chlorine bond is intact, the ^{1}H NMR of the chloride and aqua complexes with 4DHBP or 6DHBP displayed identical chemical shifts in 1 M $NaHCO_3$/D_2O solution (Supporting Information Figure S15). Thus, our collective data based on single-crystal X-ray analysis, pK_a determination, spectroscopic data, and ^{1}H NMR studies indicate that complexes $[\mathbf{1}{-}\mathbf{Cl}]^{+}$, $[\mathbf{1}{-}\mathbf{OH_2}]^{2+}$, $[\mathbf{2}{-}\mathbf{Cl}]^{+}$, and $[\mathbf{2}{-}\mathbf{OH_2}]^{2+}$ predominantly exist as their doubly deprotonated $[Cp^*Co(DHBP{-}2H^{+})(OH_2)]$ forms in 1 M $NaHCO_3$.

Carbon Dioxide Hydrogenation with $[Cp^*Co(DHBP)\text{-}L]^{n+}$ in Water. CO_2 hydrogenation with the $[Cp^*Co(DHBP)\text{-}(L)]^{n+}$ complexes in aqueous bicarbonate solutions (using a 1:1 mixture of CO_2 and H_2) was carried out under varied temperatures and pressures (H_2/CO_2). To optimize the reaction conditions, we examined various catalysts and base concentrations, and temperature and pressure settings (Figure 6 and Supporting Information Figures S19–21, Table S15). Table 2 summarizes the activities for the Co complexes examined in this study ($[\mathbf{1}{-}\mathbf{OH_2}]^{2+}$, $[\mathbf{1}{-}\mathbf{Cl}]^{+}$, $[\mathbf{2}{-}\mathbf{OH_2}]^{2+}$, $[\mathbf{2}{-}\mathbf{Cl}]^{+}$, $[\mathbf{3}{-}\mathbf{OH_2}]^{2+}$, and $[\mathbf{3}{-}\mathbf{Cl}]^{+}$). Complexes $[\mathbf{1}{-}\mathbf{Cl}]^{+}$ and $[\mathbf{1}{-}\mathbf{OH_2}]^{2+}$ (2 μmol) afforded direct hydrogenation of CO_2 to formate in 1 M $NaHCO_3$ aqueous solutions. The similar catalytic activity of $[\mathbf{1}{-}\mathbf{Cl}]^{+}$ and $[\mathbf{1}{-}\mathbf{OH_2}]^{2+}$ is not surprising because both compounds exist in their deprotonated forms as $[\mathbf{1'}{-}\mathbf{OH_2}]$ at that pH. The production of HCO_2^{-} (formate) was detected (15–24 mM) with a maximum TOF of 39 h^{-1} at 80–100 °C and 4 MPa within 1–2 h. To our knowledge, these results represent the first example of a nonphosphine Co(III) complex that can mediate CO_2 hydrogenation under aqueous conditions without any addition of organic solvents. It should

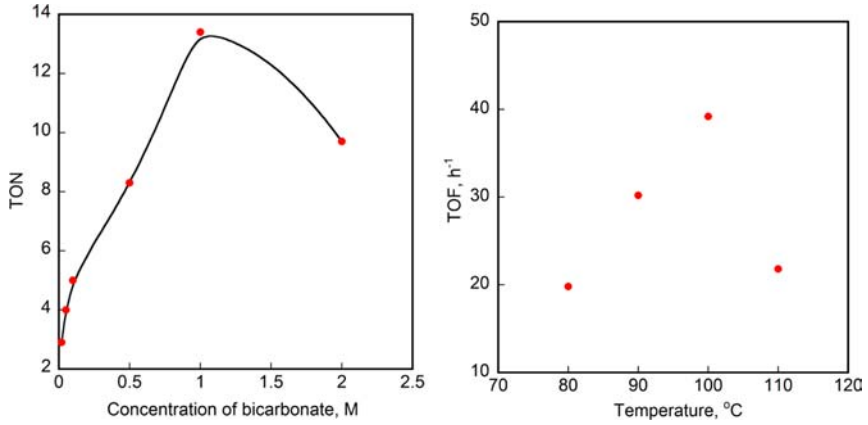

Figure 6. Optimization for CO_2 hydrogenation reaction with $[\mathbf{1}{-}\mathbf{OH_2}]^{2+}$. Left: Plot of TON versus $[HCO_3^{-}]$ (5 μmol of $[\mathbf{1}{-}\mathbf{OH_2}]^{2+}$, 5 mL of sodium bicarbonate solution, 4 MPa H_2/CO_2 (1/1), 80 °C, 1 h). Right: Plot of TOF versus reaction temperature (2 μmol of $[\mathbf{1}{-}\mathbf{OH_2}]^{2+}$), 5 mL of $NaHCO_3$ (1 M), 4 MPa H_2/CO_2 (1/1), 1 h).

dx.doi.org/10.1021/ic401707u | Inorg. Chem. 2013, 52, 12576–12586

Table 2. Hydrogenation of CO_2 in $NaHCO_3$ Solutions with Co Complexes[a]

entry	cat. /μmol	conc. of $NaHCO_3$/M	temp/°C	P/MPa	time/h	conc. of formate/mM	TON	TOF/h^{-1}
1	$[\mathbf{1-OH_2}]^{2+}$/2	1	100	4	1	15.6	39	39
2	$[\mathbf{1-OH_2}]^{2+}$/2	1	100	4	2	16.9	42	21
3	$[\mathbf{1-OH_2}]^{2+}$/2	1	90	4	2	19.6	49	25
4	$[\mathbf{1-OH_2}]^{2+}$/2	1	90	4	3	18.0	45	15
5	$[\mathbf{1-OH_2}]^{2+}$/2	1	80	5	5	21.1	53	11
6	$[\mathbf{1-OH_2}]^{2+}$/2	1	80	4	7	23.6	59	8.4
7	$[\mathbf{1-OH_2}]^{2+}$/2	1	25	4	38	2.8	7.0	0.18
8	$[\mathbf{1-Cl}]^{+}$/2	1	100	4	1	14.0	35	35
9	$[\mathbf{2-OH_2}]^{2+}$/2	1	50	4	1	0.51	1.3	1.3
10	$[\mathbf{2-Cl}]^{+}$/2	0.1	50	4	1	0.49	1.2	1.2
11	$[\mathbf{3-OH_2}]^{2+}$/5	1	60	4	3	0.66	0.66	0.22
12	$[\mathbf{3-Cl}]^{+}$/5	1	60	4	3	0.66	0.66	0.22

[a]Reaction conditions: aqueous $NaHCO_3$ solution (5 mL), H_2/CO_2 (1/1).

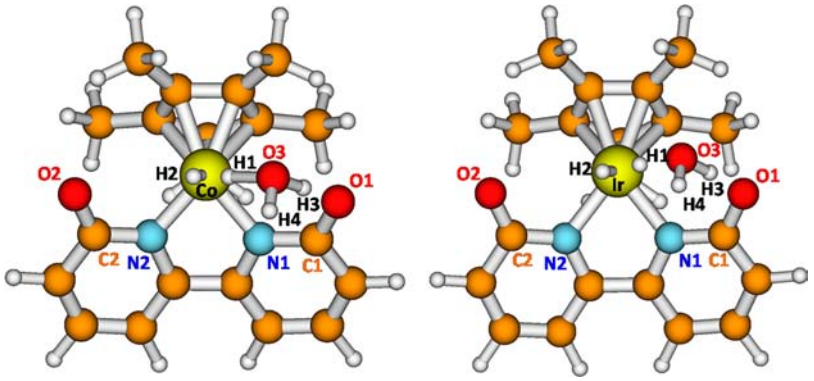

Figure 7. Comparison of the DFT-calculated transition state structures for water-assisted H_2 heterolysis via a "relayTS" for Cp*M(6DHBP−$2H^+$), M = Co and Ir, in a cpcm treatment of the water solvent. The relevant atoms are labeled the same way in the two pictures.

be noted that the use of water as a solvent medium for these cobalt complexes is critical for the catalysis, and switching to organic solvents (such as methanol, THF) did not result in detection of the formate product. For $[\mathbf{1-OH_2}]^{2+}$, the formate product was also detected at room temperature (entry 7, TOF: 0.18 h^{-1}), and increases in reaction temperature (80−100 °C) improved the reaction rate (up to 39 h^{-1}) and yields of the formate product (TON: 39−59 for 1−7 h, entries 1−6). However, catalyst decomposition was observed at temperatures >100 °C (see Figure 6) accompanied by a significant decrease in CO_2 hydrogenation activity. A meaningful activation energy could not be estimated due to the decomposition of the catalysts at higher temperatures.

In comparison to the 4DHBP complexes, the 6DHBP complexes and the nonsubstituted bpy complexes exhibited lower (TOF < 2 h^{-1}) and negligible catalytic activities, respectively (Table 2 and Supporting Information Table S15). Because complexes $[\mathbf{3-OH_2}]^{2+}$ and $[\mathbf{3-Cl}]^{+}$ do not have proton-responsive ligands, we expect lower activities for CO_2 hydrogenation. In contrast, the low activities observed for $[\mathbf{2-OH_2}]^{2+}$ and $[\mathbf{2-Cl}]^{+}$ may be due to the poor stability of these complexes under the reaction conditions. In fact, we observed the decomposition of $[\mathbf{2-OH_2}]^{2+}$ at T > 50 °C (Supporting Information Table S15). Evidently, the 6DHBP complex is less stable than the corresponding 4DHBP complex, and the steric congestion around the cobalt center may cause the decomposition (see DFT section). $[\mathbf{3-OH_2}]^{2+}$ is unstable even at room temperature in 1 M $NaHCO_3$ and decomposes completely upon heating at 50 °C for 1 h. These findings suggest that the thermal stabilities of Co 4DHBP complexes are most likely due to the strong electron-donating properties of the 4DHBP ligand;[26] however, as compared to their Ir analogues, they still decompose faster. One of the decomposition products was isolated, and structural characterization by single-crystal X-ray diffraction showed the formation of $[Co(4DHBP-H^+)_2(4DHBP)]_3[Co(4DHBP)_3](PF_6)_6$ with monodeprotonated and nondeprotonated 4DHBP ligands (Supporting Information Figure S9). Notably, we detected only a trace amount of formate with 1 M $NaHCO_3$ with catalyst $[\mathbf{1-OH_2}]^{2+}$ at 80 °C in the absence of CO_2. This suggests that introduction of CO_2 gas is necessary to increase the yield of formate unlike other cases reported.[21,30,32] These results are in agreement with our findings in the Ir DHBP systems, and our proposal that CO_2 and not bicarbonate is reduced by the catalyst.[39]

DFT Calculations. On the basis of our previous results that showed the Cp*Ir(6DHBP) complex to be more catalytically active for CO_2 hydrogenation than the Cp*Ir(4DHBP) complex,[37] we took the former species to be the prototype for exploring theoretically the lower activity of its Co analogue $[\mathbf{2-OH_2}]^{2+}$. Having established that H_2 heterolysis was the rate-determining step in CO_2 hydrogenation to formate with the Ir complexes,[37,38] we searched for a relatively low-energy water-assisted H_2 heterolysis "relayTS" transition state comparable to that we found for Cp*Ir(H···H···OH_2)-(6DHBP−$2H^+$) (where "6DHBP−$2H^+$" indicates a doubly deprotonated 6DHBP) (see Figure 7 and Table 3). We found such a transition state to exist for the Co complex, with geometric properties close to those of the Ir analogue, but occurring somewhat later along the reaction coordinate as

dx.doi.org/10.1021/ic401707u | Inorg. Chem. 2013, 52, 12576−12586

Table 3. Comparison of Calculated Geometric Properties of Cp*M(6DHBP−2H$^+$), M = Co and Ir, Water-Assisted H_2 Relay Transition States Cp*M(H···H···OH_2)(6DHBP−2H$^+$) in Aqueous Solution[a]

property	Co TS	Ir TS
M−H1 (Å)	2.066	2.036
M−H2 (Å)	1.575	1.688
H1−H2 (Å)	0.947	0.994
H1−O3 (Å)	1.309	1.359
O3−H3 (Å)	1.063	1.041
O3−H4 (Å)	0.981	0.981
H3−O1 (Å)	1.413	1.481
H2−O2 (Å)	2.910	3.011
M−N1 (Å)	1.988	2.139
M−N2 (Å)	1.956	2.121
C1−O1 (Å)	1.291	1.287
C2−O2 (Å)	1.264	1.264
H1−M−H2 (deg)	25.93	29.09
M−H1−O3 (deg)	142.47	145.19
M−H1−O3−H3 (deg)	−13.59	−21.27
H1−O3−H3−O1 (deg)	−5.53	−3.07
ν_i (cm^{-1})	1000.29i	981.02i
$\Delta G^{\ddagger}$ (kcal/mol)	8.23	9.62

[a]Atoms are labeled as in Figure 7. The free energies of activation are relative to Cp*M(6DHBP−2H$^+$) in kcal/mol at pH 8.3.

shown in Figure 7, where the two structures are compared. Key geometric and activation parameters of the two transition state structures are listed in Table 3. The free energy of activation is calculated to be somewhat lower for the Co relayTS than for the Ir relayTS when starting from $H_{2(g)}$, $H_2O_{(liq)}$, and the 5-coordinate (i.e., coordinatively unsaturated) Cp*M(6DHBP−2H$^+$). However, unlike the Ir analogue, the 5-coordinate Cp*Co(6DHBP−2H$^+$) complex is predicted to bind a solvent H_2O molecule in the sixth coordination position by 16.4 kcal/mol prior to H_2 coordination. It should be noted that the structurally characterized [Cp*Co(OH_2)(4DHBP−2H$^+$)] (i.e., [**1′−OH$_2$**]) shows a water molecule coordinated to the cobalt center (Figure 2). The free energy of the relayTS (i.e., [Cp*Ir(H···H···OH_2)(6DHBP−2H$^+$)] is raised by this amount when the Co aquo complex is taken as a reactant (as presented in Table 4 and Supporting Information Table S16). It is possible that the H_2O bound at the sixth coordination position actually becomes the bridging water in the relayTS upon attack by H_2 on the metal center (Figure 8). The Co(6DHBP) complex also exhibits a somewhat more distorted bpy ligand. This is especially true for the "heteroTS" Co complex shown in Supporting Information Figure S23, where it is compared to the much less distorted Ir heteroTS complex. The key geometric parameters of both heteroTS complexes are listed in Supporting Information Table S17.

These results prompt us to speculate that, like its Ir analogue, the Co 6DHBP complex is intrinsically more reactive than the corresponding 4DHBP complex, perhaps so much so that geometrical distortion during the initial stages of reaction may cause it to decompose. The 4DHBP complex, which has no pendent base available to assist H_2 heterolysis, may be less intrinsically reactive, but more stable, especially at higher temperatures.

To confirm that H_2 heterolysis is the rate-determining step in CO_2 hydrogenation by the Co 6DHBP catalyst, we also calculated the absolute free energies of the Cp*Co(H)-

Table 4. Calculated Energetics of Various Cp*Co(6DHBP−2H$^+$) Complexes at the B3LYP/6-31++G(d,p) 5d Using the CPCM Solvation Model with UAHF Radii

cobalt complex	reservoir	rel. G^*_{tot}[b]
Cp*Co(OH_2)(6DHBP−2H$^+$)	$H_{2(g)}$, $CO_{2(g)}$	0.00
Cp*Co(6DHBP−2H$^+$)	$H_{2(g)}$, $CO_{2(g)}$, $H_2O_{(liq)}$	16.41
Cp*Co(H···H···OH_2)(6DHBP−2H$^+$) relayTS[a]	$CO_{2(g)}$	24.64
Cp*Co(H···H)(6DHBP−2H$^+$) heteroTS[a]	$CO_{2(g)}$, $H_2O_{(liq)}$	31.79
Cp*Co(H)(6DHBP−H$^+$)	$CO_{2(g)}$, $H_2O_{(liq)}$	13.11
Cp*Co(H···CO_2)(6DHBP−2H$^+$)$^-$ TS[a]	$H^+_{(aq)}$, $H_2O_{(liq)}$	16.77
Cp*Co(OCHO)(6DHBP−2H$^+$)$^-$	$H^+_{(aq)}$, $H_2O_{(liq)}$	9.44
Cp*Co(OH_2)(6DHBP−2H$^+$)	$H^+_{(aq)}$, $HCO_2^-{}_{(aq)}$	1.58

[a]Imaginary frequencies of transition states for H_2O-assisted H_2 heterolysis and unassisted H_2 heterolysis are 1000.29i and 970.51i, respectively. The imaginary frequency of the transition state for CO_2 insertion into the Co−H bond is 38.65i. [b]Free energy relative to Cp*Co(OH_2)(6DHBP−2H$^+$), $H_{2(g)}$, and $CO_{2(g)}$ in kcal/mol at pH 8.3.

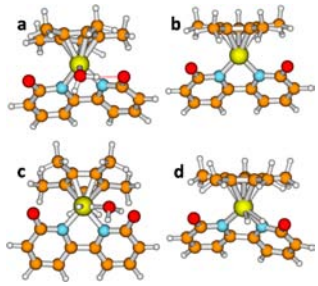

Figure 8. Cp*Co(6DHBP−2H$^+$) complexes and transition states: (a) Cp*Co(OH_2)(6DHBP−2H$^+$); (b) Cp*Co(6DHBP−2H$^+$); (c) the relayTS, Cp*Co(H···H···OH_2)(6DHBP−2H$^+$); and (d) the heteroTS, Cp*Co(H···H)(6DHBP−2H$^+$).

(6DHBP−H$^+$), the transition state for CO_2 insertion into the Co−H bond, and the Cp*Co(OCHO)(6DHBP−2H$^+$)$^-$ species. Table 4 lists the free energies of all of the intermediates in the catalytic cycle to produce the formate anion and a proton in aqueous solution at pH 8.3 relative to the Co aquo complex and a reservoir initially consisting of a molecule of $H_{2(g)}$ and a molecule of $CO_{2(g)}$. A more detailed breakdown of the contributions to the energetics is presented in Supporting Information Table S16. Supporting Information Figure S24 shows the data in Table 4 presented as a free-energy profile along the reaction coordinate. As various species are added to (or removed from) the catalyst complex, they are removed from (or added to) the reservoir, as indicated in the table. When the initial state of the catalyst complex is regenerated at the completion of the cycle, the initial $H_{2(g)}$ and $CO_{2(g)}$ in the reservoir have been converted to $H^+_{(aq)}$ and $HCO_2^-{}_{(aq)}$ with a calculated free energy change of 1.58 kcal/mol (Figure 9). The transition state for CO_2 insertion into the Co−H bond resembles a formate complex bound through the H atom to the metal center (see Supporting Information Figure S25), similar to the hydride transfer transition state found by Yang[35] in calculations of CO_2 hydrogenation by a Co−PNP catalyst. The activation free-energy transition state from the hydride complex Cp*Co(H)(6DHBP−H$^+$) is much smaller than that for H_2 heterolysis from the aqua complex Cp*Co(OH_2)(4DHBP−

dx.doi.org/10.1021/ic401707u | Inorg. Chem. 2013, 52, 12576−12586

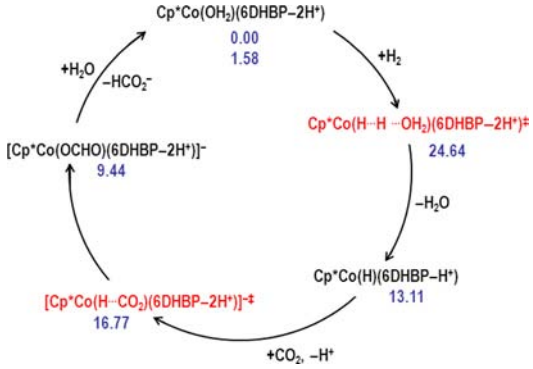

Figure 9. Proposed mechanism of hydrogenation of CO_2 by complex $Cp^*Co(OH_2)(6DHBP-2H^+)$. Computed free energies at pH 8.3 are indicated in units of kcal mol^{-1} relative to 1 M $Cp^*Co(OH_2)(6DHBP-2H^+)$ in aqueous solution and 1 atm H_2 and CO_2 gases. The calculated change in free energy around the cycle is 1.58 kcal/mol.

$2H^+$), confirming that the heterolysis of H_2 is the rate-determining step.

Dihedral angles (deg) in cobalt(III) bpy complexes in this study and the related iridium complex investigated by Papish et al. are shown in Table 5. The two rings of the bipyridine and

Table 5. Dihedral Angles (deg) in Cobalt(III) bpy and DHBP Complexes in This Study and Related Iridium Complexes

complex	two pyridine rings in bpy	(Cp*) and bpy(OH)$_2$ rings	ref
[**1−Cl**]PF_6 (**A**)	9.36(12)	38.45(9)	this work
[**1′−OH$_2$**]	3.32(4)	60.03(7)	this work
[**1−Cl**]PF_6 (**B**)	1.09(6)	49.57(10)	this work
[**3−Cl**]SO_3CF_3	13.13(12)	39.15(5)	this work
[**3−Cl**]PF_6	4.6(3)	41.7(2)	this work
[**2″−NCMe**]PF_6	18.3(2)	29.8(2)	this work
[**2−Cl**]BAr^F	16.3(4)	30.4(3)	this work
[Cp*Ir(Cl)(6DHBP)] BAr^F	14.05	36.03	43
relayTS[a]	26.61	34.21	this work
heteroTS[a]	27.49	28.47	this work

[a]Geometries of the complex are determined by DFT calculations.

hydroxy-substituted bipyridine ligands in the complexes reported in this work display dihedral angles, which range from 1.09(6)° in [**1−Cl**]PF_6 (**B**) to 16.3(4)° in [**2−Cl**]BAr^F. The dihedral angle between the two rings of the bpy ligand ranges between 1.09(6)° and 13.13(12)° in the complexes containing the bpy and 4DHBP ligand but is much larger in the complexes containing 6DHBP (i.e., 18.3(2)° and 16.4(4)°). While the dihedral angles could be affected by crystal packing effects, the dihedral angles for the 6DHBP complexes are larger in the calculated transition states than those found in the crystal structures of [**2″−NCMe**]PF_6 and [**2−Cl**]BAr^F, indicating that the 6DHBP complexes have steric problems associated with the small cobalt radii in the coordination sphere. In comparison, the Ir analogues appear to have smaller dihedral angles. Furthermore, the dihedral angles between the plane of the Cp* and the 12-membered bpy ligand are equal to or larger in the complexes containing 4DHBP than in those containing bpy. These angles are the smallest in complexes containing 6DHBP. These results suggest that the 6DHBP complexes may decompose easily due to steric strain.

CONCLUSIONS

We have synthesized a series of new $[Cp^*Co(III)(L)(DHBP)]^{n+}$ complexes and investigated their activity toward CO_2 hydrogenation under aqueous conditions. Although the noble iridium-based DHBP complexes exhibit superior activities and efficiencies for CO_2 hydrogenation in water relative to their cobalt analogues, the appreciable activities found using Cp*Co(4DHBP) complexes are promising as earth-abundant metal catalysts. While [**1−Cl**]$^+$ and [**1−OH$_2$**]$^{2+}$ can hydrogenate CO_2 to formate in 1 M $NaHCO_3$ with a maximum TOF of 39 h^{-1} at 80−100 °C, lower and negligible activity were observed from Cp*Co(6DHBP) ([**2−Cl**]$^+$ and [**2−OH$_2$**]$^{2+}$) and their nonsubstituted analogues ([**3−Cl**]$^+$ and [**3−OH$_2$**]$^{2+}$), respectively. The low TOFs observed for Co 6DHBP and Co bpy complexes were attributed to the poor thermal stability of these catalysts at the optimized temperature. Furthermore, we have illustrated that the Cp*Co(III) DHBP complexes exist predominantly as the isolable $[Cp^*Co(DHBP-2H^+)(OH_2)]$ species in 1 M $NaHCO_3$ solution. The strong electron-donating ability of the deprotonated (i.e., dianionic) 4DHBP ligand imparts better stability and activity than the bpy ligand in these cobalt complexes. Future work will target the electrocatalytic reduction of CO_2 by these water-stable Co DHBP complexes in aqueous solutions.

EXPERIMENTAL SECTION

General. All synthetic reactions were carried out under an argon atmosphere using standard Schlenk techniques or in a glovebox, and all aqueous solutions were degassed prior to use. NMR spectra were recorded at room temperature on a Bruker Avance spectrometer operating at 400 MHz for ^1H and ^{13}C, respectively. Chemical shifts are reported in parts per million (ppm) referenced to the residual solvent peak for ^1H and solvent peak for ^{13}C NMR, respectively. The J values are ±0.5 Hz. pH values were measured on a Fisher Scientific "accumet" Micro glass electrode after calibration with standard buffer solutions. Electronic absorption spectra were recorded with a UV−visible Agilent 8453 diode-array spectrophotometer and were corrected for the background spectrum of the solvent. Electrospray ionization mass spectra (ESI−MS) were acquired with a Thermo Finnigan mass spectrometer. Elemental analyses were performed by Robertson Microlit Laboratories elemental analyzer. Research grade CO_2 (>99.999%) and H_2 (>99.9999%) or mixed gas (CO_2/H_2 = 1/1) through O_2 trap was used for CO_2 hydrogenation; formate concentrations were monitored by HPLC on an anion-exclusion column (Tosoh TSKgel SCX(H+)) using aqueous H_3PO_4 solution (20 mM) as eluent and a UV detector (λ = 210 nm). Water used in the reactions was obtained from a Simplicity water purification system or a Milli-Q water purification system. 4DHBP,[22] 6DHBP,[37] and [**3−OH$_2$**]$^{2+}$ were synthesized according to literature procedures.[44,45] All other chemicals were procured from commercial sources. Additional synthetic schemes, catalytic tables and plots, spectroscopic data, DFT calculations, and X-ray single crystal diffraction studies are shown in the Supporting Information.

Synthesis of $[Cp^*CoCl_2]_2$. The synthesis was adapted from the literature.[46] Under an argon atmosphere, a Schlenk flask was charged with brown/red crystals of $Cp^*Co(CO)_2$ (5 g, 20 mmol) and dissolved in 60 mL of ether to give a brown solution. Chlorine gas was then carefully bubbled in the flask with a vented outlet needle for ca.

dx.doi.org/10.1021/ic401707u | Inorg. Chem. 2013, 52, 12576−12586

10 min. The resultant green solution was stirred for 30 min under the chlorine blanket. A green precipitate was formed, which was filtered off under air and washed with ether (twice with 10 mL) and dried under vacuum to give 5 g (94%) of the product. Purity was determined by IR and ^{1}H NMR in D_2O as previously reported.

*Synthesis of [Cp*Co(4DHBP)(Cl)]PF_6 ([**1−Cl**]PF_6).* The free 4DHBP ligand (0.28 g, 1.6 mmol) was added to a blue solution of $[Cp^*CoCl_2]_2$ (0.40 g, 0.75 mmol) in an 80 mL (1:3) mixture of water and methanol. The mixture was stirred for 2 h at 50 °C to give a dark purple solution. The solution was concentrated under air and reduced to 1 mL of volume and the extracts were taken back in 20 mL of water. The solution was filtered on a fine frit to remove insoluble materials. The resultant clear purple solution was pipetted to a saturated solution of NH_4PF_6, and upon cooling at 5 °C for a few hours a purple crystalline powder precipitated. The purple solid product was filtered, collected, and dried under vacuum overnight to give 700 mg of [**1−Cl**]PF_6 (72% yield). The compound is air and water stable for days; however, it was kept in the glovebox for long storage purposes. Purple crystals suitable for X-ray diffraction were obtained from dilute solutions of [**1−Cl**]PF_6 in water with a small amount of methanol as cosolvent at 5 °C. Crystallization of [**1−Cl**]PF_6 in 1 M $NaHCO_3$ solution at 5 °C and X-ray analysis showed the formation of [**1′−Cl**]PF_6. ^{1}H NMR (400 MHz, D_2O): δ 9.39 (d, J = 6.8 Hz, 2H (DHBP)), 7.71 (d, J = 2.8 Hz, 2H (DHBP)), 7.40 (d, J = 6.8 Hz, 2H (DHBP)), 1.25 (s, 15H, Cp*). ^{1}H NMR (400 MHz, D_2O/NaOD): δ 8.78 (t, J = 6.8 Hz, 2H (DHBP)), 7.12 (d, J = 2.8 Hz, 2H (DHBP)), 6.80 (d, J = 6.8 Hz, 2H (DHBP)), 1.12 (s, 15H, Cp*). ^{13}C NMR (400 MHz, MeOD): δ = 170.55, 158.95, 155.89, 117.75, 112.54, 95.98, 9.20. ESI−MS(+): m/z 417.1 $[M]^+$, 381.2 $[M-Cl-H]^+$, 282.1$[M-DHBP]^+$. Anal. Calcd: C, 42.69; H, 4.12; N, 4.98. Found: C, 42.76 (0.07%); H, 3.78 (0.34%); N, 4.88 (0.10%).

*Synthesis of [Cp*Co(4DHBP)(OH$_2$)](PF$_6$)$_2$ ([**1−OH$_2$**](PF$_6$)$_2$).* [**1−Cl**]PF_6 (0.22 g, 0.39 mmol) was dissolved in 100 mL of water, and solid $TlPF_6$ (0.300 g, 0.86 mmol) was added and the solution was stirred for 3 h. A purple precipitate crashed out of solution, which was filtered and washed twice with 2 mL of water and dried under a vacuum to give 165 mg (61% yield) of [**1−OH$_2$**]$(PF_6)_2$. ^{1}H NMR (400 MHz, D_2O): δ 8.98 (d, J = 8 Hz, 2H (DHBP)), 7.24 (d, J = 2 Hz, 2H (DHBP)), 6.98 (d, J = 8 Hz, 2H (DHBP)), 1.23 (s, 15H, Cp*). ^{1}H NMR (400 MHz) of [**1−OH$_2$**]$(PF_6)_2$ in (D_2O/NaOD) is identical to [**1−Cl**]PF_6, indicating ready dissociation of Cl^- ligand and exchange with water in basic solution. ^{13}C NMR (400 MHz, D_2O/KOD): δ = 176.41, 157.73, 152.08, 119.7, 113.75, 92.03, 7.94. UV−vis (H_2O or 1 M $NaHCO_3$): λ_{max}, nm (ε, M^{-1} cm^{-1}) 528 (940), 277 (32 635), 243 (53 308). ESI−MS(+): m/z 381.1 $[M-H_2O-H]^+$. Elemental analysis was obtained by crystallizing its chloride complex [Cp*Co(4DHBP)-(OH_2)]$(Cl)_2$. Anal. Calcd: C, 50.97; H, 5.35; N, 5.94. Found: C, 51.04 (0.07%); H, 4.89 (0.46%); N, 5.80 (0.14%).

*Synthesis of [Cp*Co(6DHBP)(Cl)]PF_6 ([**2−Cl**]PF_6).* The synthesis of [**2−Cl**]PF_6 was similar to that of complex [**1−Cl**]PF_6. The free 6DHBP ligand (150 mg, 0.797 mmol) was added as a solid to a blue solution of $[Cp^*CoCl_2]_2$ (0.20 mg, 0.38 mmol) in a 75 mL mixture of water and methanol (1:2). The mixture was heated at 50 °C for 2 h to give a dark purple solution. The solution was evaporated to dryness, and the resultant residue was extracted with 40 mL of water and filtered on a fine frit to remove unreacted solid materials. Addition of excess NH_4PF_6 and further cooling to 5 °C allowed for the precipitation of a purple powder. The product was collected and dried under a vacuum to give a dark purple brown powder as 280 mg (43%). ^{1}H NMR (400 MHz, D_2O): δ 7.78 (t, J = 8 Hz, 2H (DHBP)), 7.42 (d, J = 8 Hz, 2H (DHBP)), 6.78 (d, J = 8 Hz, 2H (DHBP)), 1.16 (s, 15H, Cp*). ^{1}H NMR (400 MHz, D_2O/NaOD): δ 7.51 (t, J = 8 Hz, 2H (DHBP)), 7.10 (d, J = 8 Hz, 2H (DHBP)), 6.40 (d, J = 8 Hz, 2H (DHBP)), 1.1 (s, 15H, Cp*). ^{13}C NMR (400 MHz, MeOD): δ = 172.76, 157.96, 142.17, 116.34, 111.64, 95.93, 9.84. ESI−MS(+): m/z 398.1 $[M-Cl+(OH_2)]^+$, 381.2 $[M-Cl-1H]^+$. UV−vis (H_2O): λ_{max}, nm (ε, M^{-1} cm^{-1}) 550 (750), 350 (10 550), 280 (7280). Anal. Calcd for $C_{20}H_{25}ClCoF_6N_2O_3P$ ([**2−Cl**]$(PF_6)\cdot H_2O$): C, 41.36; H, 4.34; N, 4.82. Found: C, 41.30 (0.06%); H, 4.38 (0.04%); N, 5.22 (0.40%).

*Synthesis of Cp*Co(6DHBP)(OH$_2$)(PF$_6$)$_2$ ([**2−OH$_2$**](PF$_6$)$_2$).* [**2−Cl**]PF_6 (0.12 g, 0.21 mmol) was dissolved in 50 mL of water, and solid $TlPF_6$ (0.0745 g, 0.21 mmol) was added and the solution was stirred for 3 h. The solution was then filtered, and the filtrate was then concentrated to about 10 mL. The solution was chilled to 5 °C, and purple crystals of the product were collected on a fine frit and dried under a vacuum to give 50 mg (34%) of [**2−OH$_2$**]$(PF_6)_2$. An alternative synthesis was developed that is higher yielding: A basic solution of 6DHBP ligand (150 mg, 0.80 mmol) dissolved in 30 mL of 0.2 M NaOH was added to the blue solution of $[Cp^*CoCl_2]_2$ (200 mg, 0.38 mmol) in 20 mL of water and was stirred for 2 h. The solution was then acidified by addition of aqueous sulfuric acid (1 M) to pH 3 and then evaporated to dryness to give a purple residue. The residue was extracted with 50 mL of water and filtered on a fine frit to remove insoluble materials. Addition of a solution of excess NH_4PF_6 and further cooling to 5 °C resulted in the precipitation of the product as a purple powder (300 mg, 57%). ^{1}H NMR (400 MHz, D_2O): δ 8.11 (t, J = 8 Hz, 2H (DHBP)), 7.89 (d, J = 8 Hz, 2H (DHBP)), 7.26 (d, J = 8 Hz, 2H (DHBP)), 1.14 (s, 15H, Cp*). ^{1}H NMR (400 MHz) of [**2−OH$_2$**]$(PF_6)_2$ in (D_2O/NaOD) is identical to that of [**2−Cl**]PF_6. ^{13}C NMR (400 MHz, MeOD): δ = 168.90, 156.71, 143.86, 116.66, 114.06, 96.50, 10.1. UV−vis in water is the same as that of [**2−Cl**]PF_6. ESI−MS(+): m/z 381.1 $([M-1H-(OH_2)]^+$. Elemental analysis was carried out for the Cl salt. Anal. Calcd for $C_{20}H_{27}Cl_2CoN_2O_4$ ([**2−OH$_2$**]Cl_2): C, 49.10; H, 5.56; N, 5.73. Found: C, 49.38 (0.28%); H, 4.96 (0.6%); N, 5.57 (0.02%).

*Synthesis of Cp*Co(bpy)(Cl)(PF$_6$) ([**3−Cl**]PF$_6$).* A solution of $[Cp^*CoCl_2]_2$ (0.20 mg, 0.38 mmol) was stirred with bpy (0.12 mg, 0.78 mmol) in 40 mL of a methanol and water (1:1) mixture and was heated at 50 °C for 1 h. The solvents were evaporated to dryness. The solution was extracted with 20 mL of water, and addition of excess NH_4PF_6 and further cooling to 5 °C resulted in the formation of purple crystals to give 310 mg (80%). Anal. Calcd: C, 45.26; H, 4.37; N, 5.28. Found: C, 44.95; H, 4.55; N, 5.57.

Typical Procedure for Hydrogenation of CO_2 with Co Complexes. To a freshly degassed $NaHCO_3$ aqueous solution (1 M, 5 mL) in a 10 mL glass autoclave was added a cobalt complex (2−5 μmol). After being purged with CO_2/H_2 (1/1) three times, the solution was warmed to 100 °C (or the temperature shown in Table 2) and stirred vigorously under 4 MPa of CO_2/H_2 (1/1) for 1 h. After the reaction, the formate concentration was determined by HPLC.

DFT Calculations. All calculated results for the Co complexes presented in this work were carried out with the Gaussian 09 suite of programs,[47] and employed the B3LYP hybrid functional[48−51] with the 6-31++G(d,p) 5d basis.[52−54] Geometry optimizations were carried out in the solution phase in water solvent, which was treated by the CPCM solvation model employing UAHF radii,[55−57] and were corrected for zero-point energy and thermal effects. As in our previous calculations on the analogous Ir complexes,[38] the contribution from the gas-phase translational entropy was omitted from the absolute free energy of all species with standard states in solution or the pure liquid solvent. All calculated data for Ir complexes quoted in the present work were taken from ref 38.

■ ASSOCIATED CONTENT

Ⓢ Supporting Information

Series of Cp*Co complexes with and without proton-responsive bpy ligands and their structures as determined by X-ray diffraction. Additional synthetic procedures and schemes, catalytic tables and plots, spectroscopic data, DFT calculations, and X-ray single crystal diffraction studies, as well as crystallographic data in CIF format. This material is available free of charge via the Internet at http://pubs.acs.org.

■ AUTHOR INFORMATION

Corresponding Authors

*E-mail: muckerma@bnl.gov.
*E-mail: himeda.y@aist.go.jp.

*E-mail: fujita@bnl.gov.

Author Contributions

[⊥]These authors contributed equally.

Notes

The authors declare no competing financial interest.

■ ACKNOWLEDGMENTS

Y.H. and W.-H.W. thank the Japan Science and Technology Agency (JST), ACI-C for financial support. The work at BNL was carried out under contract DE-AC02-98CH10886 with the U.S. Department of Energy and supported by its Division of Chemical Sciences, Geosciences, & Biosciences, Office of Basic Energy Sciences. Some of the calculations were performed on the computing facilities of the BNL Center for Functional Nanomaterials. Y.H., J.T.M., and E.F. designed the project. Y.M.B., W.-H.W., and J.F.H. carried out experimental investigations, D.J.S. solved X-ray structures, and J.T.M. performed DFT calculations.

■ REFERENCES

(1) United Nations Development Programme. United Nations Department of Economic and Social Affairs, and World Energy Council (2000) World Energy Assessment: Energy and the Challenge of Sustainability (United Nations Development Programme, New York).

(2) Jacobson, M. Z. *Energy Environ. Sci.* **2009**, *2*, 148−173.

(3) Arakawa, H.; Aresta, M.; Armor, J. N.; Barteau, M. A.; Beckman, E. J.; Bell, A. T.; Bercaw, J. E.; Creutz, C.; Dinjus, E.; Dixon, D. A.; Domen, K.; DuBois, D. L.; Eckert, J.; Fujita, E.; Gibson, D. H.; Goddard, W. A.; Goodman, D. W.; Keller, J.; Kubas, G. J.; Kung, H. H.; Lyons, J. E.; Manzer, L. E.; Marks, T. J.; Morokuma, K.; Nicholas, K. M.; Periana, R.; Que, L.; Rostrup-Nielson, J.; Sachtler, W. M. H.; Schmidt, L. D.; Sen, A.; Somorjai, G. A.; Stair, P. C.; Stults, B. R.; Tumas, W. *Chem. Rev.* **2001**, *101*, 953−996.

(4) Mikkelsen, M.; Jorgensen, M.; Krebs, F. C. *Energy Environ. Sci.* **2010**, *3*, 43−81.

(5) Appel, A. M.; Bercaw, J. E.; Bocarsly, A. B.; Dobbek, H.; DuBois, D. L.; Dupuis, M.; Ferry, J. G.; Fujita, E.; Hille, R.; Kenis, P. J. A.; Kerfeld, C. A.; Morris, R. H.; Peden, C. H. F.; Portis, A. R.; Ragsdale, S. W.; Rauchfuss, T. B.; Reek, J. N. H.; Seefeldt, L. C.; Thauer, R. K.; Waldrop, G. L. *Chem. Rev.* **2013**, *113*, 6621−6658.

(6) Inoue, Y.; Izumida, H.; Sasaki, Y.; Hashimoto, H. *Chem. Lett.* **1976**, 863−864.

(7) Jessop, P. G.; Ikariya, T.; Noyori, R. *Chem. Rev.* **1995**, *95*, 259−272.

(8) Wang, W.; Wang, S.; Ma, X.; Gong, J. *Chem. Soc. Rev.* **2011**, *40*, 3703−3727.

(9) Leitner, W.; Dinjus, E.; Gassner, F. In *Aqueous-Phase Organometallic Catalysis, Concepts and Applications*; Cornils, B., Herrmann, W. A., Eds.; Wiley-VCH: Weinheim, 1998; pp 486−498.

(10) Steele, B. C. H.; Heinzel, A. *Nature* **2001**, *414*, 345−352.

(11) Fukuzumi, S. *Eur. J. Inorg. Chem.* **2008**, 1351−1362.

(12) Jessop, P. G.; Joo, F.; Tai, C. C. *Coord. Chem. Rev.* **2004**, *248*, 2425−2442.

(13) Grasemann, M.; Laurenczy, G. *Energy Environ. Sci.* **2012**, *5*, 8171−8181.

(14) Enthaler, S.; von Langermann, J.; Schmidt, T. *Energy Environ. Sci.* **2010**, *3*, 1207−1217.

(15) Johnson, T. C.; Morris, D. J.; Wills, M. *Chem. Soc. Rev.* **2010**, *39*, 81−88.

(16) Columbia, M. R.; Crabtree, A. M.; Thiel, P. A. *J. Electroanal. Chem.* **1993**, *345*, 93−105.

(17) Gassner, F.; Leitner, W. *J. Chem. Soc., Chem. Commun.* **1993**, 1465−1466.

(18) Laurenczy, G.; Joó, F.; Nadasdi, L. *Inorg. Chem.* **2000**, *39*, 5083−5088.

(19) Elek, J.; Nádasdi, L.; Papp, G.; Laurenczy, G.; Joó, F. *Appl. Catal., A* **2003**, *255*, 59−67.

(20) Federsel, C.; Jackstell, R.; Boddien, A.; Laurenczy, G.; Beller, M. *ChemSusChem* **2010**, *3*, 1048−1050.

(21) Boddien, A.; Gartner, F.; Federsel, C.; Sponholz, P.; Mellmann, D.; Jackstell, R.; Junge, H.; Beller, M. *Angew. Chem., Int. Ed.* **2011**, *50*, 6411−6414.

(22) Himeda, Y. *Eur. J. Inorg. Chem.* **2007**, 3927−3941.

(23) Schmeier, T. J.; Dobereiner, G. E.; Crabtree, R. H.; Hazari, N. *J. Am. Chem. Soc.* **2011**, *133*, 9274−9277.

(24) Azua, A.; Sanz, S.; Peris, E. *Chem.-Eur. J.* **2011**, *17*, 3963−3967.

(25) Himeda, Y.; Miyazawa, S.; Hirose, T. *ChemSusChem* **2011**, *4*, 487−493.

(26) Fujita, E.; Muckerman, J. T.; Himeda, Y. *Biochim. Biophys. Acta, Bioenerg.* **2013**, *1827*, 1031−1038.

(27) Tanaka, R.; Yamashita, M.; Nozaki, K. *J. Am. Chem. Soc.* **2009**, *131*, 14168−14169.

(28) Tanaka, R.; Yamashita, M.; Chung, L. W.; Morokuma, K.; Nozaki, K. *Organometallics* **2011**, *30*, 6742−6750.

(29) Tai, C. C.; Chang, T.; Roller, B.; Jessop, P. G. *Inorg. Chem.* **2003**, *42*, 7340−7341.

(30) Federsel, C.; Boddien, A.; Jackstell, R.; Jennerjahn, R.; Dyson, P. J.; Scopelliti, R.; Laurenczy, G.; Beller, M. *Angew. Chem., Int. Ed.* **2010**, *49*, 9777−9780.

(31) Ziebart, C.; Federsel, C.; Anbarasan, P.; Jackstell, R.; Baumann, W.; Spannenberg, A.; Beller, M. *J. Am. Chem. Soc.* **2012**, *134*, 20701−20704.

(32) Federsel, C.; Ziebart, C.; Jackstell, R.; Baumann, W.; Beller, M. *Chem.-Eur. J.* **2012**, *18*, 72−75.

(33) Jeletic, M. S.; T, M. M.; Appel, A. M.; Lenehan, J. C. *J. Am. Chem. Soc.* **2013**, *135*, 11533−11536.

(34) Langer, R.; Diskin-Posner, Y.; Leitus, G.; Shimon, L. J.; Ben-David, Y.; Milstein, D. *Angew. Chem., Int. Ed.* **2011**, *50*, 9948−9952.

(35) Yang, X. Z. *ACS Catal.* **2011**, *1*, 849−854.

(36) Himeda, Y.; Onozawa-Komatsuzaki, N.; Miyazawa, S.; Sugihara, H.; Hirose, T.; Kasuga, K. *Chem.-Eur. J.* **2008**, *14*, 11076−11081.

(37) Wang, W.-H.; Hull, J. F.; Muckerman, J. T.; Fujita, E.; Himeda, Y. *Energy Environ. Sci.* **2012**, *5*, 7923−7926.

(38) Wang, W.-H.; Muckerman, J. T.; Fujita, E.; Himeda, Y. *ACS Catal.* **2013**, *3*, 856−860.

(39) Hull, J. F.; Himeda, Y.; Wang, W. H.; Hashiguchi, B.; Periana, R.; Szalda, D. J.; Muckerman, J. T.; Fujita, E. *Nat. Chem.* **2012**, *4*, 383−388.

(40) For example: (a) Du, P. W.; Eisenberg, R. *Energy Environ Sci.* **2012**, *5*, 6012−6021. (b) Andreiadis, E. S.; Jacques, P.-A.; Tran, P. D.; Leyris, A.; Chavarot-Kerlidou, M.; Jousselme, B.; Matheron, M.; Pécaut, J.; Palacin, S.; Fontecave, M.; Artero, V. *Nat. Chem.* **2013**, *5*, 48−53. (c) Artero, V.; Chavarot-Kerlidou, M.; Fontecave, M. *Angew. Chem., Int. Ed.* **2011**, *50*, 7238−66. (d) McCrory, C. C. L.; Uyeda, C.; Peters, J. C. *J. Am. Chem. Soc.* **2012**, *134*, 3164−3170. (e) Sun, Y.; Bigi, J. P.; Piro, N. A.; Tang, M. L.; Long, J. R.; Chang, C. J. *J. Am. Chem. Soc.* **2011**, *133*, 9212−9215. (f) Stubbert, B. D.; Peters, J. C.; Gray, H. B. *J. Am. Chem. Soc.* **2011**, *133*, 18070−18073. (g) Singh, W. M.; Baine, T.; Kudo, S.; Tian, S. L.; Ma, X. A. N.; Zhou, H. Y.; DeYonker, N. J.; Pham, T. C.; Bollinger, J. C.; Baker, D. L.; Yan, B.; Webster, C. E.; Zhao, X. *Angew. Chem., Int. Ed.* **2012**, *51*, 5941−5944. (h) Anxolabéhère-Mallart, E.; Costentin, C.; Fournier, M.; Nowak, S.; Robert, M.; Savéan, J.-M. *J. Am. Chem. Soc.* **2012**, *134*, 6104−6107. (i) Wiedner, E. S.; Yang, J. Y.; Dougherty, W. G.; Kassel, W. S.; Bullock, R. M.; Rakowski DuBois, M.; DuBois, D. L. *Organometallics* **2010**, *29*, 5390−5401.

(41) (a) Esswein, M. J.; Nocera, D. G. *Chem. Rev.* **2007**, *107*, 4022−4047. (b) Dempsey, J. L.; Brunschwig, B. S.; Winkler, J. R.; Gray, H. B. *Acc. Chem. Res.* **2009**, *42*, 1995−2004. (c) Schneider, J.; Jia, H.; Muckerman, J. T.; Fujita, E. *Chem. Soc. Rev.* **2012**, *41*, 2036−2051 and references therein.

(42) Kawahara, R.; Fujita, K.; Yamaguchi, R. *J. Am. Chem. Soc.* **2012**, *134*, 3643−3646.

(43) DePasquale, J.; Nieto, I.; Reuther, L. E.; Herbst-Gervasoni, C. J.; Paul, J. J.; Mochalin, V.; Zeller, M.; Thomas, C. M.; Addison, A. W.; Papish, E. T. *Inorg. Chem.* **2013**, *52*, 175−9183.
(44) Dadci, L.; Elias, H.; Frey, U.; Hornig, A.; Koelle, U.; Merbach, A. E.; Paulus, H.; Schneider, J. S. *Inorg. Chem.* **1995**, *34*, 306−315.
(45) Hong, D.; Jung, J.; Park, J.; Yamada, Y.; Suenobu, T.; Lee, Y. M.; Nam, W.; Fukuzumi, S. *Energy Environ. Sci.* **2012**, *5*, 7606−7616.
(46) Macazaga, M. J.; Delgado, S.; Medina, R. M.; Masaguer, J. R. *J. Organomet. Chem.* **1984**, *277*, 423−426.
(47) Frisch, M. J.; et al. *Gaussian 09*; Gaussian, Inc.: Wallingford, CT, 2010.
(48) Becke, A. D. *J. Chem. Phys.* **1993**, *98*, 5648−5652.
(49) Lee, C. T.; Yang, W. T.; Parr, R. G. *Phys. Rev. B* **1988**, *37*, 785−789.
(50) Vosko, S. H.; Wilk, L.; Nusair, M. *Can. J. Phys.* **1980**, *58*, 1200−1211.
(51) Becke, A. D. *Phys. Rev. A* **1988**, *38*, 3098−3100.
(52) Stevens, W. J.; Basch, H.; Krauss, M. *J. Chem. Phys.* **1984**, *81*, 6026−6033.
(53) Stevens, W. J.; Krauss, M.; Basch, H.; Jasien, P. G. *Can. J. Chem.* **1992**, *70*, 612−630.
(54) Cundari, T. R.; Stevens, W. J. *J. Chem. Phys.* **1993**, *98*, 5555−65.
(55) Klamt, A.; Schüürmann, G. *J. Chem. Soc., Perkin Trans. 2* **1993**, 799−805.
(56) Barone, V.; Cossi, M. *J. Phys. Chem. A* **1998**, *102*, 1995−2001.
(57) Cossi, M.; Rega, N.; Scalmani, G.; Barone, V. *J. Comput. Chem.* **2003**, *24*, 669−681.